Generating large topological charge Laguerre-Gaussian beam based on 4K phase-only spatial light modulator

Ruijian Li(李瑞健)[1,3], Yuan Ren(任 元)[2,4,*], Tong Liu(刘 通)[1,4], Chen Wang(王 琛)[5], Zhengliang Liu(刘政良)[1,4], Jie Zhao(赵 杰)[1,3], Rusheng Sun(孙汝生)[1,3], and Ziyang Wang(王紫阳)[6]

1 Department of Aerospace Science and Technology, Space Engineering University, Beijing 101416, China
2 Basic Ministry, Space Engineering University, Beijing 101416, China
3 Lab of Quantum Detection & Awareness, Space Engineering University, Beijing 101416, China
4 State Key Lab of Laser Propulsion & its Application, Space Engineering University, Beijing 101416, China
5 63729 Troops of Chinese People's Liberation Army, Taiyuan 030027, China
6 School of Space Information, Space Engineering University, Beijing 101416, China
**Corresponding author: renyuan_823@aliyun.com*

Received Month X, XXXX; accepted Month X, XXXX; posted online Month X, XXXX

The resolution of the Spatial Light Modulators (SLMs) screen and the encoding algorithm of the computer-generated hologram are the primary limiting factors in the generation of large topological charge vortex beams. This paper attempts to solve these problems by improving both the hardware and the algorithm. Theoretically, to overcome the limitations of beam waist radius, the amplitude profile function of large topological charge LG beam is properly improved. Then an experimental system employing a 4K phase-only SLM is set up, and the LG beams with topological charge up to 1200 are successfully generated. Furthermore, we discuss the effect of different beam waist radii on the generation of LG beams. Additionally, the function of the LG beam is further improved to generate a LG beam with a topological charge as high as 1400. Our results set a new benchmark for generating large topological charge vortex beams, which can be widely used in precise measurement, sensing, and communication.

Keywords: spatial light modulator; Laguerre-Gaussian beam; computer-generated hologram; large topological charge
DOI: 10.3788/COLXXXXXX.XXXXXX.

1. Introduction

Vortex beams (VBs) are a kind of spatially structured light field with a hollow dark core, a helical phase structure characterized by the phase factor $\exp(il\phi)$, where l denotes the topological charge and ϕ denotes the azimuthal angle. In 1992, Allen *et al.* proves that VBs under the paraxial condition can carry the well-defined orbit angular momentum (OAM) of $l\hbar$ for each photon, where $\hbar$ is the Planck constant[1]. In 1994, Allen and Barnett *et al.* prove that the OAM carried by VBs' is still $l\hbar$ by Maxwell's equation under non-paraxial conditions[2]. Since then, photons carrying OAM have gradually become known and have given rise to a wide range of research and applications. Laguerre-Gaussian (LG) mode, as a set of solutions of paraxial wave equations in cylindrical coordinates, is characterized by two main parameters, i.e., azimuthal index (topological charge) l and radial index p, and is widely used in rotational Doppler measurement [3], optical trap[4,5], optical wrench[6], atomic capture[7], particle control[8,9], to name a few.

The topological charge is an important parameter of VBs, and the generation of VBs with large topological charge are of great significance for the further improvement of various researches. Larger topological charge represents higher OAM degree of freedom. It has great applications in ultra-low speed object speed detection and optical communication[10]. In order to obtain larger topological charge, scientists have carried out a series of studies on improving the generation approaches of VBs. In 2009, Sciarrino Fabio et al. generate VBs with topological charge of 100 using the Q-plate method[11]. In 2012, Robert Fickler *et al.* generate VBs with a topological charge of ±300 using a spatial light modulator (SLM)[12]. In 2015, Chen et al. generate multi-ring nested VBs with topological charge up to 360 by SLM[13]. In 2020, Jonathan Pinnell et al. successfully generate LG beams with topological charge of 600 by explore the limits of what fields SLMs are capable of generating and detecting in the context of VBs carrying OAM[14]. However, the resolution of SLM used in this work is 1920×1080, there are some defects in the phase depth and the limit of the topological charge number of reconstructed light field. On this basis, if the resolution of SLM screen is improved, the limit value of the topological charge of LG beams can be further increased. Now the resolution of commercially available 4K liquid-crystal SLMs can reach 3840×2160, which have the potential to overcome the previous limit. In addition to the resolution of SLM, the conventional encoding method of computer-generated holograms (CGHs) is also not suitable to generate VBs with higher topological charge. The 4K SLM has been widely used in communication[15], microscopy[16], quantum information processing[17] and optical operation[18], and other fields.

In this paper, based on a 4K phase-only SLM and the method of complex amplitude modulation, LG beams with topological charge up to 1400 has been generated for the first time. We explore the core elements of the LG expressions and further simplify the LG mode expression while increasing the topological charge significantly. The topological charge has been measured precisely, which is the largest value generated and detected with SLMs that has been reported to date. Besides, the influence of beam waist radius on the quality of LG beams with different topological charges is investigated. A new scheme is proposed to further improve the limit value of the topological charge of VBs as well.

2. Method

The expression of the annular LG amplitude function with $p = 0$ can be written as[19]

$$LG_0^l(r) = \sqrt{\frac{2}{\pi |l|!}} \frac{1}{\omega_0} \left(\frac{\sqrt{2}r}{\omega_0} \right)^{|l|} \exp\left(-\frac{r^2}{\omega_0^2} \right) \tag{1}$$

where ω_0 denotes the waist radius of LG beam, the standard procedure for generating LG beams is to expand and collimate the incident laser beam so that the spot size remains constant on the SLM screen[20], then load the hologram that generates the transport function $T = LG_0^l(r)\exp(il\phi)$ on the SLM screen. However, when generating LG beams with a large topological charge, the original derivation formula of LG beams cannot produce the desired beam effects. We mention this fact and expand on it in the context of generating LG modes with a large topological charge l, according to[14]

$$LG_0^l(r) \propto \left(\frac{\sqrt{2}r}{\omega_0} \right)^{|l|} \exp\left(-\frac{r^2}{\omega_0^2} \right) \tag{2}$$

as the topological charge increases, $(r)^{|l|}$ gradually diverge to infinity. At the same time, the waist radius will gradually increase, leading to the latter term phase component gradually tending to 0. In this case, the two terms can cancel each other out. Considering the appropriate modal approximation, it is concluded that:

$$LG_0^l(r): \ \exp\left(-\frac{(r - r_l)^2}{(\omega_0/\sqrt{2})^2} \right) \tag{3}$$

Based on Eq.3, considering that the amplitude of the single-ring LG beam at the radius position of the beam is maximum, the following formula is proposed:

$$r_l = \sqrt{\frac{|l|}{n}} \omega_0 \tag{4}$$

the value range of n is set as $[1, 2]$. When $|l| \geq 100$, the error of Eq.4 will be less than 0.05%. Note that when calculating CGHs, to make full use of the phase modulation depth of the SLM, the amplitude of the field is normalized into the interval $[0, 1]$. It greatly simplifies the problem that it is very difficult to calculate the normalized factor of real LG beam amplitude by Eq.1 when the value $|l|!$ is too large.

As the topological charge of the LG beam increases, the waist radius of the beam will increase continuously while the size of the SLM screen is fixed. If the waist radius is too large, the LG mode ring will not be completely loaded on the screen. In this case, it can be compensated by scaling the embedded waist radius:

$$\omega_0 \to \frac{\omega_0}{\sqrt{m|l|+1}} \tag{5}$$

the value range of m is also set as $[1, 2]$. According to Eq.4 and Eq.5, parameters m and n are adjusted respectively according to the radius of the hologram so that the radius of the hologram ring is always smaller than the screen width. Based on reference [14], we can first set the scale coefficients as $m \to 1, n \to 2$.

In this paper, as the LG beam with a large topological charge is generated based on phase-only SLM, the complex amplitude modulation encoding method needs to be realized. The complex amplitude modulation of the light field can be expressed as:

$$s(x, y) = a(x, y)\exp\left[i\phi(x, y) \right] \tag{6}$$

where a denotes the amplitude component of the light, ϕ denotes the phase component of the light, (x, y) respectively is the number of pixels in the row and column of the SLM screen, the purpose of complex amplitude modulation is to encode $s(x, y)$ and obtain a phase-only hologram, which can be expressed as:

$$s(x, y) = \exp[i\psi(a, \phi)] \tag{7}$$

where $\psi(a, \phi)$ denotes the phase-only component encoding the amplitude and phase information, and the formula under the phase-only condition is as follows[21]:

$$\psi(\phi, a) = f(a)\sin(\phi) \tag{8}$$

In Eq.8, $f(a)$ is the independent variable function of numerical inversion under the condition of known amplitude.

Since the modulation efficiency of the SLM cannot reach 100%, a blazed grating is required to separate the modulated light from the unmodulated light. In this case, the hologram can be written as:

$$h(x, y) = \sum_{-\infty}^{+\infty} \mathrm{J}_n\left[f(a) \right] \exp\left[in\left(\phi + 2\pi k_x x + 2\pi k_y y \right) \right] \tag{9}$$

where $J_m[f(a)]$ is the m[th] order Bessel function of $f(a)$, (k_x, k_y) are the spatial frequency vectors of the shining grating in the direction (x, y) respectively.

The screen of the SLM is composed of liquid crystal, and the smaller the size of the liquid crystal is, the larger the angle of the diffraction light is. In this paper, 4K SLM is adopted, which can separate the diffraction zero-order and diffraction first-order to a greater extent, and the LG beam with a larger topological charge number can be generated theoretically. Based on the wavefront derivation formula of VBs, the SLM resolution, and laser beam wavelength, the formula for the maximum topological charge of VBs that can be generated is as follows:

$$|l|_{\max} = \frac{2\pi RNA}{\lambda} \tag{10}$$

where NA denotes the numerical aperture in optical systems, λ denotes the wavelength, R denotes the radius of the largest circle that the SLM screen can load, and the theoretical value is the width of the screen. It should be noted that there needs to be room on the SLM screen for the hologram, so the R taken in the actual experiment should be slightly less than the theory.

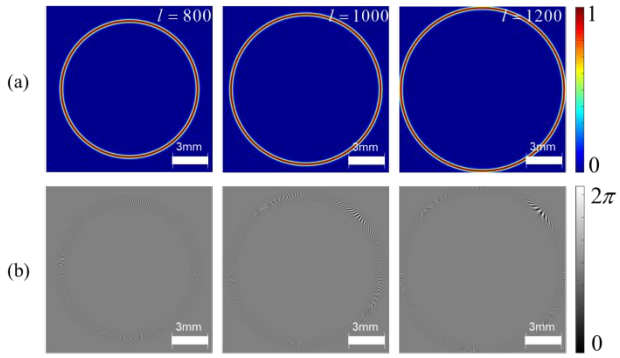

Fig.1 Amplitude and coded holograms of LG beams with topological charges of 800,1000, and 1200 (a)amplitude. (b)coded holograms.

In this paper, we use 4K phase-only SLM with resolution 3840×2160 and pixel size $3.74\mu m$, and the wavelength of the He-Ne laser used is $633nm$. In the experiment, the lens we used is 25.4mm in diameter and has a focal length of 150mm. The refractive index of air is $k = 1$, so the value of NA is 0.084. According to the formula mentioned above, the maximum topological charge that the 4K SLM can realize can be calculated as:

$$|l|_{\max} \approx 3368 \tag{11}$$

According to Eq.9, as the diffraction order of modulated and unmodulated light is separated, an aperture is usually used to prevent the unmodulated beam from propagating along with the optical system, which limits the NA in Eq.10 and the limit value of the topological charge $|l|_{\max}$. As compensation, the distance between diffraction orders can be widened by increasing the frequency of diffraction gratings. However, due to the limitations of SLM screen resolution and phase modulation depth, a large grating frequency greatly reduces the quality of the reconstructed light field.

The simulated amplitude of the LG beam and corresponding coded holograms are shown in Fig.1. Fig.1(a) shows the amplitude of LG beams with topological charges of 800, 1000, and 1200, respectively. Fig.1(b) shows the holograms obtained with corresponding topological charges.

3. Experiment

Fig. 2 shows the experimental setup for generating LG beam with a large topological charge by 4K phase-only SLM. In Fig.2(a), the 632.8nm Gaussian beam is generated by a He-Ne laser. A telescope system comprising an objective and a positive lens L1 is formed for beam expansion and collimation. The beam then passes through the polarizer Pol and the non-polarized beam-splitting prism NPBS and enters the 4K phase-only SLM. The hologram for large topological charge LG beam generation is loaded on the LCD screen. Then the modulated light passes through the NPBS again, and the Fourier transform is implemented through the lens L2. A CCD is used to observe and analyze the beam profile. In Fig.2(b), the holograms loaded onto the SLM are changed. To measure the topological charge of LG beams, an additional annular plane-wave beam with ring-shaped amplitude distribution is introduced to the hologram. After the first-order diffraction passes through the aperture, the interference pattern between the LG beam and the annular plane wave can be collected after the reflection of a mirror and lens L3, from which the topological charge of the LG beam can be inferred.

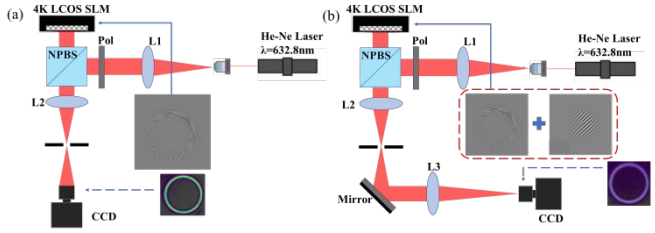

Fig.2 The experimental setup of a large topological charge LG beam generated by 4K SLM (L1, L2, L3: lens, Pol: polarization, SLM: phase-only spatial light modulators, NPBS: non-polarizing beam splitter). (a)generation of LG beams. (b) interference of LG beams and annular plane waves.

Although the manufacturing technology of SLMs has been advanced, the SLM's LCD screen is not completely flat, which results in the quality of the reconstructed light field being affected, and the effect becomes more obvious as the light field propagates. An assumption can be made in this case, the larger the area occupied by a LG beam on the hologram, the larger the wavefront distortion of the reconstructed light field will be. Therefore, the most

intuitive way to minimize the wavefront error is to minimize the hologram area, but this method cannot eliminate the wavefront error because with the decrease of the beam size, the pixelation approximation of the transfer function encoded by the hologram deteriorates. At the same time:

$$\theta \propto \frac{\lambda}{\pi\omega_0} \tag{12}$$

where θ denotes the far-field divergence angle of VB. According to Eq.12, it can be concluded that θ is inversely proportional to the optical waist radius ω_0. In the hologram, the smaller the beam size is, the larger the size of the generated beam in the far field will be. Under the diffraction condition of the blazed grating, the light field of second-order diffraction will also influence the quality of the first-order diffraction light field to a certain extent. In this experiment, the waist radius is adjusted according to the experimental results to achieve the optimal quality of the large topological charge LG beam. The modulation range of waist radius is between 5mm and 12mm, among which 12mm is the screen width of 4K SLM used in the experiment.

Corresponding to the simulation in Fig.1, the CGH is loaded on the 4K SLM, and LG beams with topological charges of 800, 1000, and 1200 are experimentally generated, as shown in Fig.3. The large topological charge singlet LG beam in Fig. 3(a) and the interference pattern in Fig. 3(b) are acquired by CCD in Fig. 2(a) and Fig. 2(b), respectively. Through the experimental results, it can be seen that with the increase of the topological charge number, the intensity distribution of the rings is becoming increasingly uneven, which is because $s(x,y)=\exp[\mathrm{i}\psi(\phi,a)]$ in Eq.7 only applies in the continuous limit, due to the small pixels of SLM, the CGHs displayed by it are discrete. Such pixelated distribution will lead to more and more different OAM modes being introduced into the field with the increase of topological charge under the condition that the resolution remains unchanged, which has a significant effect on the amplitude distribution of the beam, resulting in its intensity biased to one side of the LG ring, while this problem will become more obvious with the increase of topological charges.

Based on the LG beam hologram loaded on SLM, the phase information of circular ring plane wave modulated by amplitude is introduced[22] to realize coaxial interference between VB and plane wave, and the petal-shaped interference pattern was obtained as shown in Fig. 3(b), the resulting interferogram is composed of $|l|$ "petals". These petal modes were then magnified, and segments of the beam were captured using a CCD camera. An image processing script is written to determine the arc angle of collecting arc fragments and calculate the number of petals, from which we can estimate the total number of petals which is the topological charge $|l|$ of the LG beam. In this paper, the number of petals is detected by the interference pattern of the LG beam with a topological charge difference of 50. The arc angle of the interference pattern shown in Fig. 4(a) is taken to obtain the curve shown in Fig. 4(b). It can be seen from Fig. 4(c) that although there is a slight error in the calculation of the petal number, the size of the topological charge number corresponding to the LG beam can be obtained more accurately.

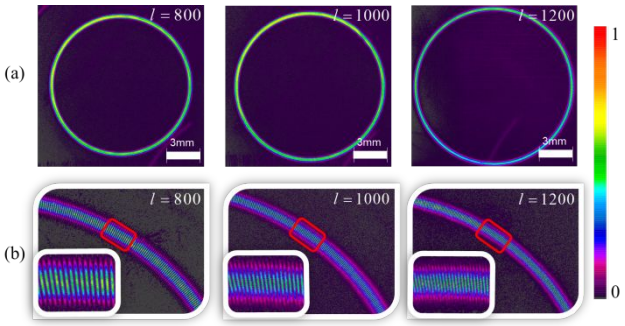

Fig.3 Experimental results of LG beams with topological charges of 800,1000, and 1200 (a) singlet LG beam. (b) plane wave interference pattern.

As the waist radius ω_0 changed in the experiment, the line graph of LG beam quality changes with the increase of topological charges was calculated and compared with the theoretical value, as shown in Fig. 5(a). The quality of the generated large topological charge LG beam is determined by the correlation coefficient C between the intensity distribution of the reconstructed light field generated by the experiment and the target light field. Which is defined as:

$$C=\frac{\sum_m\sum_n(A_{mn}-\bar{A})(B_{mn}-\bar{B})}{\sqrt{\left(\sum_m\sum_n(A_{mn}-\bar{A})^2\right)\left(\sum_m\sum_n(B_{mn}-\bar{B})^2\right)}} \tag{13}$$

where (m,n) denotes the number of pixels in length and width of the strength section, A_{mn} and B_{mn} are respectively the intensity of the experimentally generated each pixel of the large topological charge LG beam and the simulated LG beam, $\bar{A}$ and $\bar{B}$ are the average intensity of the generated beam and the simulated beam respectively. The value range of C is $[0,1]$, the higher the value of C is, the higher the similarity between the generated beam and the simulated beam is. It can be seen that with the increase of topological charge, the overall quality of the LG beam decreases due to the introduction of more and more OAM modes in the generated beam. At the same time, the change of waist radius will also affect the beam quality, so the adjustment of waist radius has certain limitations. When the beam size is small, there will be fewer pixels that can effectively represent the transmitted azimuth phase

function $LG(r)\exp(il\phi)$, resulting in faster degradation of the quality of OAM mode.

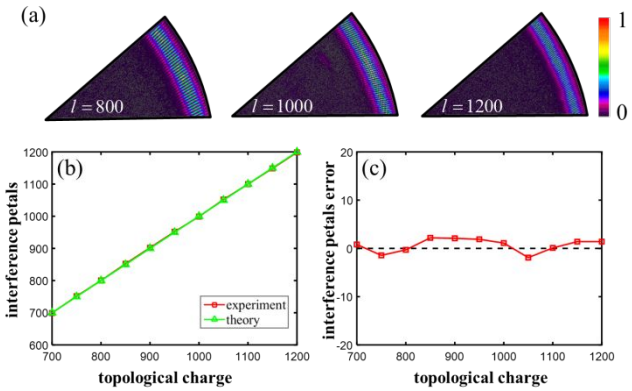

Fig.4 (a) Data processing collected interference pattern arc fragments. (b) Experimental and theoretical graphs of topological charge number and interference petal number of LG beam. (c) The curve of interference petal error with topological charge

We also give the simulation and experimental intensity cross-sections of LG beams with topological charges of 800,1000, and 1200, as shown in Fig.5(b) and (c). It can be seen that the overall trend is in good agreement, indicating that the generated LG beams quality is good.

After achieving the topological charge limit of the method in reference [14] above, consider further improving the topological charge of the generated LG beam. Change the values of the scaling coefficients n and m in Eq.4 and Eq.5. The value of m gradually approaches 2, and the value of n gradually approaches 1 with the increase of the topological charge number l of the LG beam, ensuring that the LG beam in the hologram always maintains the maximum screen size of the SLM while reducing the value n while expanding m , which can maximize the resolution of 4K SLM. Based on this, the topological charge number of the reconstructed light field was further improved, and the LG beam with a topological charge as high as 1400 was successfully generated while $m = 1.35, n = 1.6$, as shown in Fig. 6. It can be seen from Fig. 6(a1)-(a6) that as the number of topological charges increases, the problem of mode crosstalk becomes more and more serious. The intensity distribution of the generated LG beam is more and more biased to one side, while the halo area of the reconstructed light field increases, and the diffraction VB of the second-order and the first order will have cross-interference, which seriously affects the beam quality of the reconstructed light field. The resolution of the spatial light modulator also affects the grating constant introduced in the complex amplitude modulation and the clarity of interference petals when the topological charge number is large, but the waist radius is small. These are the limiting factors for the generation and detection of VBs with larger topological charges.

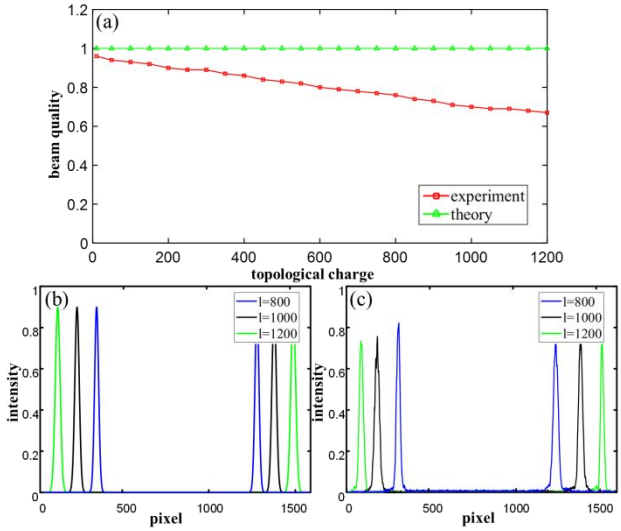

Fig.5 (a) Quality variation of LG beam versus topological charge. (b) The section distribution of simulated intensity of LG beams with topological charges of 800,1000, and 1200. (c) The section distribution of LG beam experimental intensity at corresponding topological charges.

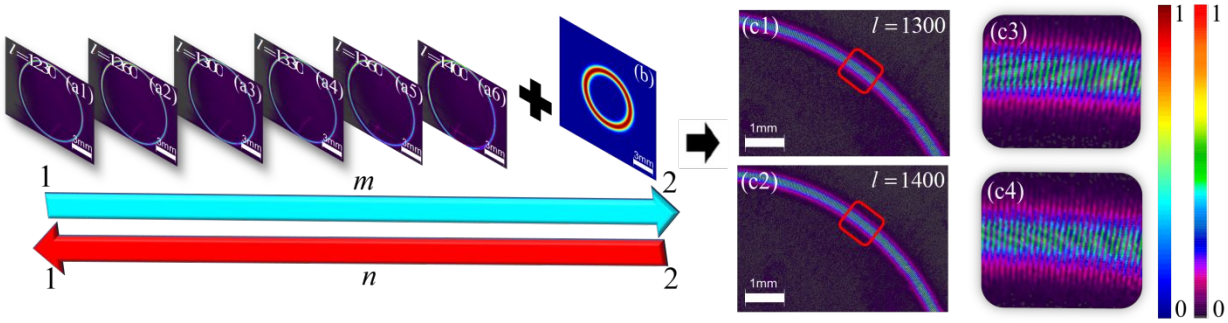

Fig.6. (a1-a6) Singlet LG beams with topological charges in the range 1200-1400. (b) Annular plane waves modulated by complex amplitude. (c1-c2) LG beam interference patterns with topological charges of 1300 and 1400. (c3-c4) Partial enlargement of LG beam interference patterns with topological charges of 1300 and 1400.

Based on the singlet LG beam, it interferes with an annular plane wave, as shown in Fig. 6(b), to produce a petal-like fringe, and the pattern is shown in Fig. 6(c1)-(c2), the partial enlargement of the interference patterns under the corresponding topological charge is shown in Fig. 6 (c3)-(c4). It should be emphasized that Fig. 6(a6) corresponds to

the LG model with a topological charge number $l = 1400$, which is the maximum generated and detected by the SLM reported so far. However, it should be noted that the LG beam mode modified by Eq. 4 and Eq.5 is more complex and is not a real LG beam.

Anyway, the LG beam generated in this paper also has some limitations and problems. First, the beam is derived from the conventional LG formula by modal approximation, in which case the reconstructed light field is not a completely accurate LG mode. Second, there is a radial node p in Laguerre polynomials. The formula used in this paper ignores the existence of radial nodes because the introduction of radial nodes will increase the complexity and uncontrollability of the modal approximation formula. Therefore, the radial section $p = 0$ is uniformly set in the paper. This also leads to the inability to generate multi-ring nested LG beams with large topological charges, which requires further improvement in the algorithm in the future.

4. Conclusion

Firstly, the traditional LG beam formula is modally approximated and derived in detail. The reconstructed light field is modulated by complex amplitude. The intensity distributions of LG beams with topological charges of 800, 1000, and 1200 are simulated. Secondly, relevant experimental devices are built to achieve the generation of large topological charge LG beams. At the same time, the annular plane wave interference is introduced to accurately measure the topological charge number, and the variation of LG beam amplitude fidelity with topological charges is discussed. Based on this, the LG beam modal approximation formula is further improved, and the LG beam with $l = 1400$ topological charges is successfully prepared, which is also the VB with the largest topological charge generated by SLM. It provides a new scheme for further improving the limit value of the topological charge of VB, which is of great significance in weak speed measurement and communication.

This work was supported by the National Natural Science Foundation of China (Nos. 62173342 and 61805283), Key research projects of foundation strengthening program（No. 2019-JCJQ-ZD）

References

1. L Allen, M W Beijersbergen, R J C Spreeuw and J P Woerdman. Orbital angular momentum of light and the transformation of Laguerre-Gaussian laser modes[J]. Phys. Rev. A. 1992, 45(11):8185.
2. S M Barnett and L Allen. Orbital angular momentum and nonparaxial light beams[J]. Opt. Commun. 1994, 110(5-6):670-678.
3. Y Ding, Y S Ding, S Qiu, T Liu and Y Ren. Rotational frequency detection of spinning objects at general incidence using vortex beam (Invited)[J]. Infrared Laser Eng. 2021, 50(9): 20210451.
4. M J Snadden, A S Bell, R B M Clarke, E Riis and D H Mcintyre. Doughnut mode magneto-optical trap[J]. J. Opt. Soc. Am. B. 1997,14,544.
5. J Arlt, T Hitomi and K Dholakia. Atom guiding along Laguerre-Gaussian and Bessel light beams[J]. Appl. Phys. B. 2000,71,549.
6. S Franke-Arnold, L Allen and M Padgett. Advances in optical angular momentum[J]. Laser Photonics Rev. 2008,2,299.
7. F K Fatemi and M Bashkansky. Cold atom guidance using a binary spatial light modulator[J]. Opt. Express. 2006,14,1368.
8. D S Bradshaw and D L Andrews. Interactions between spherical nanoparticles optically trapped in Laguerre-Gaussian modes[J]. Opt. Lett. 2005,22,3039-3041.
9. A V Nesterov and V G Niziev. Laser beams with axially symmetric polarization[J]. J. Phys. D: Appl. Phys. 2000,33,1817-1822.
10. Wang, Z., N. Zhang, and X. C. Yuan. High-volume optical vortex multiplexing and de-multiplexing for free-space optical communication[J].Opt. Express. 2011, 19(2):482-492.
11. E Nagali, F Sciarrino, F D Martini, L Marrucci, B Piccirillo, E Karimi and E Santamato. Quantum Information Transfer from Spin to Orbital Angular Momentum of Photons[J]. Phys. Rev. Lett. 2009, 103(1):013601.
12. R Fickler, R Lapkiewicz, WN Plick, M Krenn, C Schaeff, S Ramelow and A Zeilinger. Quantum Entanglement of High Angular Momenta[J]. Science. 2012, 338(6107):640-643.
13. Chen L, Zhang W, Lu Q and Lin X. Making and identifying optical superpositions of high orbital angular momenta[J]. Phys. Rev. A. 2013, 88(5):4019-4019.
14. J Pinnell, V Rodriguez-Fajardo and A Forbes. Probing the limits of orbital angular momentum (OAM) generation and detection with spatial light modulators[J]. J. Opt. 2020, 23(1): 015602
15. J Wang. Data information transfer using complex optical fields: a review and perspective (Invited Paper) [J]. Chin. Opt. Lett. 2017, 15(3):16-20.
16. C Maurer, A Jesacher, S Bernet and M Ritsch-Marte. What spatial light modulators can do for optical microscopy[J]. Laser Photonics Rev. 2011, 5(1):81-101.
17. M Mirhosseini, O S Magaña-Loaiza, M N O'Sullivan, B Rodenburg, M Malik, M P J Lavery, M J Padgett, D J Gauthier and R W Boyd. High-dimensional quantum cryptography with twisted light[J]. New J. Phys. 2014, 17(3):033033.
18. D G Grier, Y Han. Erratum: Vortex rings in a constant electric field [J]. Nature. 2003, 424 (267-268)
19. Taro Ando, Yoshiyuki Ohtake, Naoya Matsumoto, Takashi Inoue, and Norihiro Fukuchi. Mode purities of Laguerre – Gaussian beams generated via complex-amplitude modulation using phase-only spatial light modulators[J]. Opt. Lett. 2009, 34(1):1-3
20. C Rosales-Guzmán and A Forbes. How to shape light with spatial light modulators (SPIE,2017) p. 57.
21. V Arrizón, U Ruiz, R Carrada and L A González. Pixelated phase computer holograms for the accurate encoding of scalar complex fields[J]. J. Opt. Soc. Am. A. 2007, 24(11):3500– 3507.
22. C Wang, Y Ren, T Liu, Z L Liu, S Qiu, Y Ding, J Zhao and R J Li. Mode analyzer for known optical vortices from a spatial light modulator with collinear holography[J]. Appl. Opt. 2021, 60(31):9706-9712.